Balanced Multiplicative Regularization for the Contrast Source Inversion Method

Amer Zakaria[1], Colin Gilmore[2], Steven Pistorius[2] and Joe LoVetri[1]

[1]Department of Electrical and Computer Engineering
University of Manitoba, Winnipeg, MB, R3T 5V6, Canada
azakaria@ee.umanitoba.ca, Joe_LoVetri@umanitoba.ca

[2]Medical Physics
CancerCare Manitoba, Winnipeg, MB, R3T 0V9, Canada
cgilmore@ee.umanitoba.ca, stephen.pistorius@cancercare.mb.ca

Abstract: A balanced multiplicative regularization for the contrast source inversion method is proposed to account for the imbalance between the real and imaginary parts of the contrast for an unknown object-of-interest (OI). The real and imaginary updates due to multiplicative regularization are scaled differently using a balancing factor determined empirically. Experimental data are inverted using the proposed method where it is shown that the new method is successful in reconstructing the real and imaginary components of the contrast more accurately in comparison to the conventional multiplicative regularization method.

Keywords: Contrast Source Inversion, Multiplicative Regularization, Microwave Imaging.

1. Introduction

In some microwave imaging applications, the object-of-interest's (OI) complex relative permittivity constitutes are out-of-balance. This results in most inversion algorithms favoring, unintentionally, the reconstruction of the real part of the OI over the imaginary part, with the reconstruction of the later being erratic.

A state-of-the-art algorithm that has had much success in solving inverse scattering problems is the contrast source inversion method [1]. The outcome of the CSI algorithm can be enhanced by incorporating an L_2-norm total variation multiplicative regularization (MR) [2]. Herein an improvement to the multiplicative regularization applied to CSI is proposed. The enhancement accounts for the imbalance that can occur between the real and imaginary components of the OI's contrast. The scaling factor in the balanced multiplicative regularization is dependent on the ratio of the real to the imaginary components' magnitude of the OI. The proposed method is motivated by the success of a pre-scaled multiplicative regularizer for the Gauss-Newton inversion algorithm [3].

In this paper, we consider a two-dimensional (2D) transverse magnetic (TM) problem with $z-$polarized electric field and an $\exp(j\omega t)$ time dependence; however the proposed method can be readily applied to 2D transverse electric (TE) and three-dimensional (3D) problems.

2. Problem Formulation

We consider a 2D problem domain Ω that contains an imaging domain $\mathcal{D}$. An isotropic, non-magnetic OI is located within $\mathcal{D}$ and is surrounded by a background medium of known electrical properties, ϵ_b. The electrical contrast of the OI is defined as $\chi(\vec{r}) \triangleq (\epsilon_r(\vec{r}) - \epsilon_b(\vec{r}))/\epsilon_b(\vec{r})$ where ϵ_r is the unknown complex relative permittivity of the OI; here $\vec{r} = (x, y)$ is a 2D position vector. Outside $\mathcal{D}$, $\chi(\vec{r}) = 0$.

One of total T transmitters produce a time-harmonic $z-$polarized TM electromagnetic field. In the absence of the OI, the sources radiate an incident field E_t^{inc}, where the subscript t denotes the active transmitter index. A total field E_t is produced and is measured at R observation points per transmitter located on a measurement surface $\mathcal{S}$. The scattered field E_t^{sct} resulting from the difference in the electrical properties of the OI and the background medium is defined as $E_t^{\text{sct}} \triangleq E_t - E_t^{\text{inc}}$. The scattered field is governed by the following scalar Helmholtz equation:

$$\nabla^2 E_t^{\text{sct}}(\vec{r}) + k_b^2(\vec{r}) E_t^{\text{sct}}(\vec{r}) = -k_b^2(\vec{r}) w_t(\vec{r}) \tag{1}$$

where $k_b(\vec{r}) = \omega\sqrt{\mu_0 \epsilon_0 \epsilon_b(\vec{r})}$ is the background wavenumber, and $w_t(\vec{r}) \triangleq \chi(\vec{r}) E_t(\vec{r})$ is the contrast source. The solution for this partial differential equation requires that appropriate boundary conditions be imposed on the surface enclosing the problem domain Ω.

3. Inversion Algorithm

A. Contrast Source Inversion

In the contrast source inversion (CSI) algorithm, the two unknown variables, the contrast sources w_t and the contrast χ, are updated with an interlaced application of the conjugate gradient algorithm to minimize the following cost functional [1]:

$$\begin{aligned} \mathcal{C}^{\text{CSI}}(\chi, w_t) =& \mathcal{C}^{\mathcal{S}}(w_t) + \mathcal{C}^{\mathcal{D}}(\chi, w_t), \\ =& \frac{\sum_t \left\| u_t(\vec{r}) - \mathcal{G}_{\mathcal{S}}\left\{w_t\right\} \right\|_{\mathcal{S}}^2}{\sum_t \left\| u_t(\vec{r}) \right\|_{\mathcal{S}}^2} + \frac{\sum_t \left\| \chi(\vec{r}) E_t^{\text{inc}}(\vec{r}) - w_t(\vec{r}) + \chi(\vec{r}) \mathcal{G}_{\mathcal{D}}\left\{w_t\right\} \right\|_{\mathcal{D}}^2}{\sum_t \left\| \chi(\vec{r}) E_t^{\text{inc}}(\vec{r}) \right\|_{\mathcal{D}}^2} \end{aligned} \tag{2}$$

where u_t is the measured scattered field on a measurement surface $\mathcal{S}$ for each transmitter, $\mathcal{G}_{\mathcal{S}}$ is the data operator and $\mathcal{G}_{\mathcal{D}}$ is the domain operator. The data operator returns the scattered field on a measurement surface $\mathcal{S}$ given the contrast source variable w_t, while the domain operator returns the scattered field in the imaging domain $\mathcal{D}$ from the contrast source variable w_t.

The first step in CSI is updating the contrast source variable (w_t) using the conjugate gradient (CG) method with Polak-Ribière search directions; here the contrast (χ) variable is assumed constant. Next, holding the contrast source variable constant, the functional becomes quadratic with respect to the contrast variable; therefore the contrast variable can be updated analytically such that the functional is minimized. The two steps are performed sequentially at each iteration of the CSI algorithm until the solution converges [1].

B. Balanced Multiplicative Regularization for CSI

A successful regularization technique that has been used with CSI is the weighted L_2-norm total variation multiplicative regularization (MR) [2]. For applications where there is an imbalance between the real and imaginary components of the contrast, the application of MR to CSI can result in an erroneous reconstruction of the imaginary part, as the inversion algorithm will inadvertently

favor the real part of the contrast. This can be improved by scaling the real and imaginary updates of the contrast in the MR constraint differently, as proposed in [3]. Essentially, by modifying the MR term, the imbalance in the contrast can be compensated to achieve a reconstruction that is more accurate for both the real and imaginary parts of the contrast. The balanced multiplicative regularization (BMR) term is given as

$$\begin{aligned}\mathcal{C}_n^{\mathrm{BMR}}(\chi) &= \int_{\mathcal{D}} b_n(\vec{r})^2 \big(|\nabla\chi_{\mathrm{R}}(\vec{r})|^2 + Q^2|\nabla\chi_{\mathrm{I}}(\vec{r})|^2 + \delta_n^2\big)\, d\vec{r} \\ &= \|b_n(\vec{r})\nabla\chi_{\mathrm{R}}(\vec{r})\|_{\mathcal{D}}^2 + \|b_n(\vec{r})Q\nabla\chi_{\mathrm{I}}(\vec{r})\|_{\mathcal{D}}^2 + \delta_n^2\,\|b_n(\vec{r})\|_{\mathcal{D}}^2\,.\end{aligned} \tag{3}$$

Here χ_{R} and χ_{I} are the real and imaginary components of the contrast, Q is a balancing factor, and

$$b_n(\vec{r}) = \Big(A\big(|\nabla\chi_{\mathrm{R},n-1}(\vec{r})|^2 + Q^2|\nabla\chi_{\mathrm{I},n-1}(\vec{r})|^2 + \delta_n^2\big)\Big)^{-1/2}. \tag{4}$$

where A is the total area of domain $\mathcal{D}$ and $\delta_n^2 = \mathcal{C}^{\mathcal{D}}(\chi_{n-1}, w_{t,n})\,\bar{A}^{-1}$ in which χ_{n-1} is the BMR-CSI update of the contrast variable at the $n-1$ iteration and $\bar{A}$ is the mean area of the numerical cells in the reconstruction domain $\mathcal{D}$.

With the inclusion of balanced multiplicative regularization term, the objective functional at the n^{th} iteration becomes

$$\mathcal{C}_n(\chi, w_t) = \mathcal{C}_n^{\mathrm{BMR}}(\chi) \times \mathcal{C}^{\mathrm{CSI}}(\chi, w_t). \tag{5}$$

Since $\mathcal{C}_n^{\mathrm{BMR}}(\chi_{n-1}) = 1$, the update procedure for the contrast source variable w_t remains unchanged; however, this is not the case for the contrast variable χ. The real and imaginary components of the contrast, χ_{R} and χ_{I}, are updated independently in BMR-CSI. The analytical CSI update for the contrast variables is no longer performed in BMR-CSI, rather the real and imaginary components of the contrast are updated by a conjugate-gradient method as follows:

$$\begin{aligned}\chi_{\mathrm{R},n} &= \chi_{\mathrm{R},n-1} \;+ \alpha_n^{\chi_{\mathrm{R}}}\, d_n^{\chi_{\mathrm{R}}} \\ \chi_{\mathrm{I},n} &= \chi_{\mathrm{I},n-1} \;+ \alpha_n^{\chi_{\mathrm{I}}}\, d_n^{\chi_{\mathrm{I}}}.\end{aligned} \tag{6}$$

The search directions $d_n^{\chi_{\mathrm{R}}}$ and $d_n^{\chi_{\mathrm{I}}}$ are calculated using the Polak-Ribière search directions, and are given by

$$\begin{aligned}d_n^{\chi_{\mathrm{R}}} &= -g_n^{\chi_{\mathrm{R}}} + \frac{\big\langle g_n^{\chi_{\mathrm{R}}}, g_n^{\chi_{\mathrm{R}}} - g_{n-1}^{\chi_{\mathrm{R}}}\big\rangle_{\mathcal{D}}}{\big\|g_{n-1}^{\chi_{\mathrm{R}}}\big\|_{\mathcal{D}}^2}\; d_{n-1}^{\chi_{\mathrm{R}}} \\ d_n^{\chi_{\mathrm{I}}} &= -g_n^{\chi_{\mathrm{I}}} + \frac{\big\langle g_n^{\chi_{\mathrm{I}}}, g_n^{\chi_{\mathrm{I}}} - g_{n-1}^{\chi_{\mathrm{I}}}\big\rangle_{\mathcal{D}}}{\big\|g_{n-1}^{\chi_{\mathrm{I}}}\big\|_{\mathcal{D}}^2}\; d_{n-1}^{\chi_{\mathrm{I}}}\end{aligned} \tag{7}$$

where $g_n^{\chi_{\mathrm{R}}}$ and $g_n^{\chi_{\mathrm{I}}}$ are the preconditioned gradients of $\mathcal{C}_n(\chi, w_t)$ with respect to χ_{R} and χ_{I} respectively and are given by

$$\begin{aligned}g_n^{\chi_{\mathrm{R}}} &= \Big(-2\,\nabla\cdot b_n^2\nabla\chi_{\mathrm{R},n-1} \times \mathcal{C}^{\mathrm{CSI}}(\chi_{n-1}, w_{t,n}) + g_{\mathcal{D},n}^{\chi_{\mathrm{R}}} \times \mathcal{C}^{\mathrm{BMR}}(\chi_{n-1})\Big)\; P_n \\ g_n^{\chi_{\mathrm{I}}} &= \Big(-2\,\nabla\cdot Q^2 b_n^2\nabla\chi_{\mathrm{I},n-1} \times \mathcal{C}^{\mathrm{CSI}}(\chi_{n-1}, w_{t,n}) + g_{\mathcal{D},n}^{\chi_{\mathrm{I}}} \times \mathcal{C}^{\mathrm{BMR}}(\chi_{n-1})\Big)\; P_n.\end{aligned} \tag{8}$$

Here the preconditioner $P_n = \big(\sum_t |E_{t,n}|^2\big)^{-1}$ where $E_{t,n} \triangleq E_t^{\mathrm{inc}} + \mathcal{G}_{\mathcal{D}}\{w_t\}$ is the total field for transmitter t and

$$\begin{aligned}g_{\mathcal{D},n}^{\chi_{\mathrm{R}}} &= \mathrm{Re}\big(2\eta_{\mathcal{D},n-1}\sum_t E_{t,n}^* r_{t,n}\big) \\ g_{\mathcal{D},n}^{\chi_{\mathrm{I}}} &= \mathrm{Im}\big(2\eta_{\mathcal{D},n-1}\sum_t E_{t,n}^* r_{t,n}\big)\end{aligned} \tag{9}$$

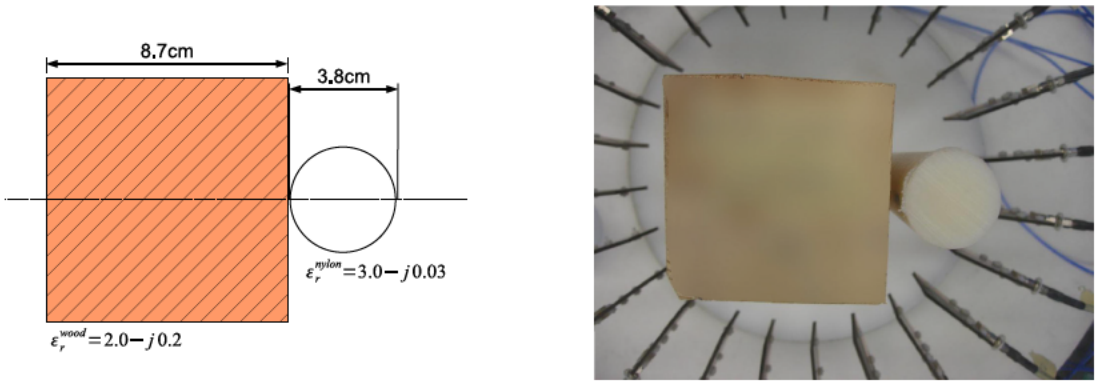

Fig. 1. The OI consisting of a wooden block and a nylon cylinder.

where $\eta_{\mathcal{D},n-1}$ is the reciprocal of the normalization factor for $\mathcal{C}^{\mathcal{D}}$ and , $r_{t,n} = \chi_{n-1}E_{t,n} - w_{t,n}$ is the residual of the domain equation at the n^{th} iteration after updating the contrast source variable, w_t. The update step-sizes $\alpha_n^{\chi\text{R}}$ and $\alpha_n^{\chi\text{I}}$ in (6) are calculated analytically based on the following minimization:

$$\begin{aligned} \alpha_n^{\chi\text{R}} &= \arg\min_{\alpha^{\chi\text{R}}} \left\{\mathcal{C}_n\left(w_{t,n}\,, \chi_{\text{R},n-1} + \alpha^{\chi\text{R}}\, d^{\chi\text{R},n}\,, \chi_{\text{I},n-1}\right)\right\} \\ \alpha_n^{\chi\text{I}} &= \arg\min_{\alpha^{\chi\text{I}}} \left\{\mathcal{C}_n\left(w_{t,n}\,, \chi_{\text{R},n-1}\,, \chi_{\text{I},n-1} + \alpha^{\chi\text{I}}\, d^{\chi\text{I},n}\right)\right\}, \end{aligned} \tag{10}$$

which involves finding the roots of two cubic polynomials. This yields one real root along with a complex-conjugate pair for each polynomial; the real roots are the step-sizes [2].

4. Inversion Results

The BMR-CSI algorithm is tested by inverting an experimental dataset collected using our air-filled MWI system. The full description of the MWI system and the calibration procedure are outlined in [4]. The system is air-filled ($\epsilon_b = 1$) with 24 Vivaldi antennas used as transmitters and receivers. The Vivaldi antennas are evenly distributed on a circle of radius 0.1345 m. For each transmitter, 23 measurements were collected; thus the total number of measurements in the dataset is $23 \times 24 = 522$. The dataset was acquired at a frequency $f = 3$ GHz.

The dielectric phantom used consists of a wooden block and a nylon cylinder as depicted in figure 1 (a) and (b). The relative complex permittivities are $\epsilon_r^{\text{wood}} = 2.0 - j0.2$ and $\epsilon_r^{\text{nylon}} = 3.0 - j0.03$ at a frequency $f = 3$ GHz. They were measured using the Agilent 85070E dielectric probe kit. The imaging domain $\mathcal{D}$ is selected to be a square centered in the problem domain Ω with side length equal to 0.24 m. The calibrated measurements are inverted using MR-CSI and BMR-CSI formulated using the finite-element method (FEM) [5,6]. The number of unknowns in $\mathcal{D}$ is 4522 and they are located at the nodes of an unstructured triangular mesh. The MR-CSI reconstructions are shown in figure 2 (a) and (b), along with the BMR-CSI results for $Q = 20$ in figure 2 (c) and (d).

The reconstruction results for the real component of the OI are similar using either MR-CSI or BMR-CSI; both algorithms predicted the real component of the OI accurately. Using MR-CSI the imaginary part reconstruction is not satisfactory; on the other hand, with BMR-CSI for $Q = 20$ the algorithm reconstructs the imaginary component of the dielectric constant for the wooden block properly with an average value of 0.11 for $-\text{Im}(\epsilon_r)$; this is less than the value measured by the

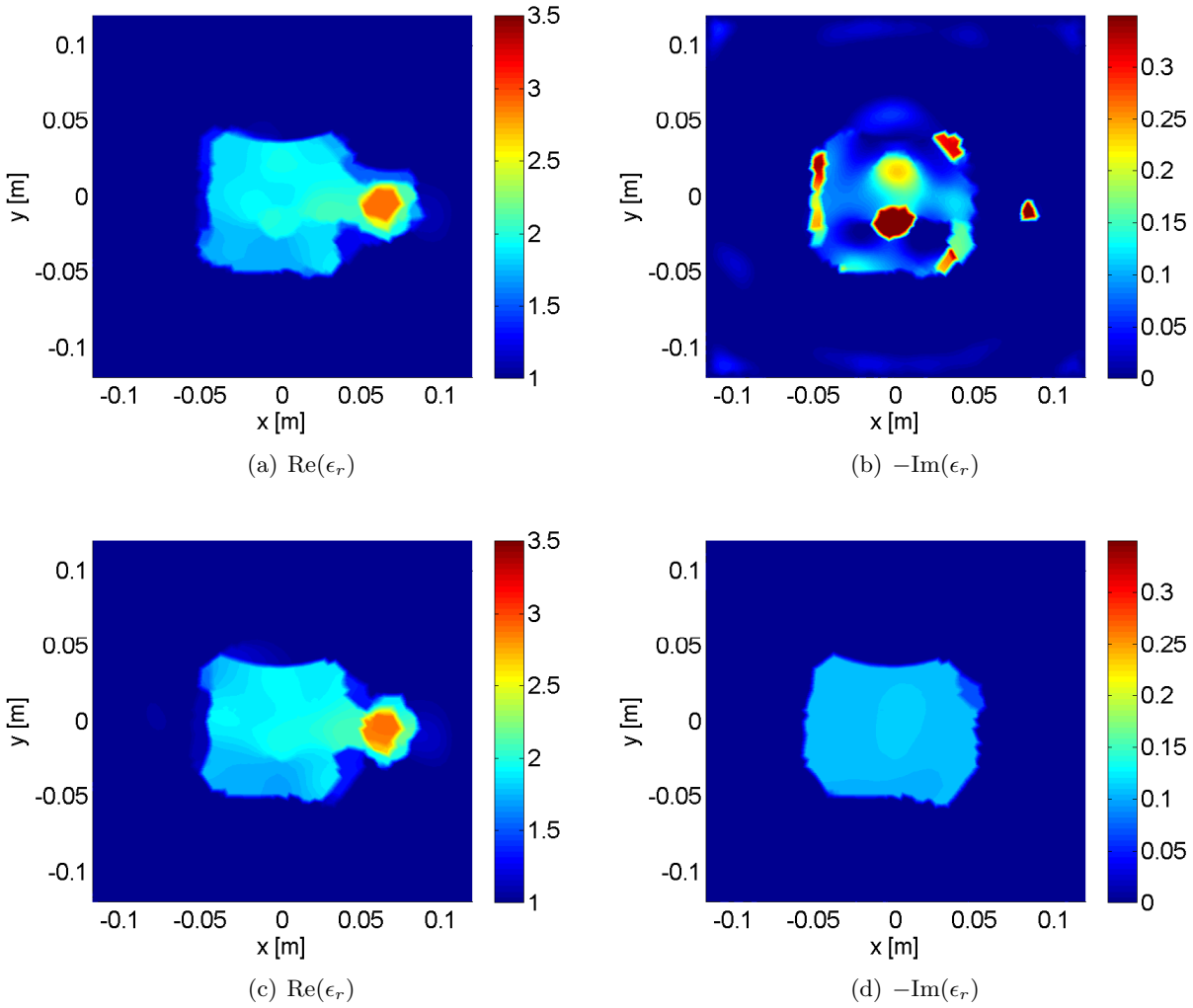

(a) $\mathrm{Re}(\epsilon_r)$ (b) $-\mathrm{Im}(\epsilon_r)$

(c) $\mathrm{Re}(\epsilon_r)$ (d) $-\mathrm{Im}(\epsilon_r)$

Fig. 2. The reconstructions at a frequency $f = 3$ GHz using (a)-(b) MR-CSI and (c)-(d) BMR-CSI for $Q = 20$.

dielectric probe. As for the nylon cylinder, considering it is almost lossless and the MWI system used has a limited signal-to-noise ratio as well as dynamic range, the reconstruction of the cylinder's imaginary part is difficult. We note here that the reconstruction obtained herein is very similar to that of the balanced version of GNI, PMR-GNI [3].

5. Conclusion

We have demonstrated that BMR-CSI can provide a better reconstruction of the imaginary part of the relative complex permittivity when there is a large imbalance between the real and imaginary parts of the OI's electrical properties. The balancing factor has been selected empirically. A future improvement would be to automate the selection of the scaling factor as well as to vary the Q values across the imaging domain region.

6. Acknowledgment

The authors acknowledge the financial support of NSERC, MITACS, CancerCare Manitoba, the Western Economic Diversification Canada and the University of Manitoba.

7. References

[1] P. M. van den Berg and R. E. Kleinman, "A contrast source inversion method," *Inverse Problems*, vol. 13, pp. 1607-1620, December 1997.

[2] P. M. van den Berg, A. Abubakar and J. Fokkema, "Multiplicative regularization for contrast profile inversion," *Radio Science*, vol. 38, no. 2, pp. 23 (1-10), 2003.

[3] P. Mojabi and J. LoVetri, "A pre-scaled multiplicative regularized Gauss-Newton inversion," *Antennas and Propagation, IEEE Transcations on*, vol. 59, no. 8, pp. 2954-2963, August 2011.

[4] C. Gilmore, P. Mojabi, A. Zakaria, M. Ostadrahimi, C. Kaye, S. Noghanian, L. Shafai, S. Pistorius, and J. LoVetri, "A wideband microwave tomography system with a novel frequency selection procedure," *Biomedical Engineering, IEEE Transcations on*, vol. 57, no. 4, pp. 894-904, April 2010.

[5] A. Zakaria, C. Gilmore and J. LoVetri, "Finite-element contrast source inversion method for microwave imaging," *Inverse Problems*, vol. 26, no. 11, p. 115010, 2011.

[6] A. Zakaria and J. LoVetri, "Application of multiplicative regularization to the finite-element contrast source inversion method," *Antennas and Propagation, IEEE Transcations on*, vol. 59, no. 9, pp. 3495-3498, September 2011.